



## Full Length Research Article

### ARGON ADSORPTION BEHAVIOR OF MULTI-WALLED CARBON NANOTUBES WITH DIFFERENT DIAMETERS

<sup>1,2\*</sup>Diana, A., <sup>1</sup>Zoro Diana, E. G., <sup>1</sup>Grafoute, M., <sup>3</sup>Manu, V., <sup>1</sup>Yebouet, A. F., <sup>1</sup>Guehi, F. J. and <sup>3</sup>Bajaj, H. C.

<sup>1</sup>Condensed Matter and Technology Laboratory, Felix Houphouet Boigny University of Cocody- Abidjan, Côte d'Ivoire

<sup>2</sup>International University of Grand-Bassam, STEM, Bassam, Côte d'Ivoire

<sup>3</sup>Discipline of Inorganic Materials and Catalysis (DIMC), CSMCRI, Bhavnagar, India

#### ARTICLE INFO

##### Article History:

Received 28<sup>th</sup> June, 2016  
Received in revised form  
26<sup>th</sup> July, 2016  
Accepted 16<sup>th</sup> August, 2016  
Published online 30<sup>th</sup> September, 2016

##### Key Words:

Multi-walled carbon nanotubes,  
Nitric acid, Argon, BET surface area,  
Adsorption properties, Transmission electron  
microscopy, Adsorption capacity, Gas storage.

#### ABSTRACT

Multi-walled carbon nanotubes (MWCNT) with two different average diameters were purified with the nitric acid (MWCNT-HNO<sub>3</sub>) treatment process. The N<sub>2</sub> (adsorption/desorption) measurement showed an increase in surface area from the raw material to the MWCNT 4 normal (4N) acid (HNO<sub>3</sub>) treatment material, and a decrease in surface area from the MWCNT-4N acid treatment material to the MWCNT-8N acid treatment material. Transmission electron microscopy (TEM) analysis implies that some amorphous carbons have been removed from the treated samples and defects on the sidewalls were observed. We conducted a study of the adsorption of argon onto multi-walled carbon nanotubes of different diameters, using the volumetric method. The specific surfaces were measured by the BET method; the calculation of the adsorption capacity and energy were made. The analysis of these parameters revealed that the surface area, the adsorption capacity and the adsorption energy are inversely proportional to the diameter of MWCNT. Those results were compared to the adsorption of hydrogen onto the MWCNT. We found that the results do not match and conclude that argon cannot be stored on MWCNT.

*Copyright*©2016, Diana et al. This is an open access article distributed under the Creative Commons Attribution License, which permits unrestricted use, distribution, and reproduction in any medium, provided the original work is properly cited.

#### INTRODUCTION

Since their discovery, carbon nanotubes (CNTs) (Ijima, 1991) have attracted enormous interest because of their unique mechanical, thermal, optical, chemical, and electronic properties (Mahalingan *et al.*, 2012; Tu *et al.*, 2012; Su *et al.*, 2012; Salehi *et al.*, 2012; Nasir Mahmood *et al.*, 2013). The CNTs composed of one graphite sheet are called single-walled carbon nanotubes (SWCNTs), and those which are composed of more than one graphite sheet are called multi-walled carbon nanotubes (MWNTs) (Nalwa, 1994). One goal in CNT research is to obtain pure samples. Therefore, methods of purification have evolved from arc discharge to acid treatments (Mahalingan *et al.*, 2012; Tu *et al.*, 2012; Su *et al.*, 2012; Salehi *et al.*, 2012; Nasir Mahmood *et al.*, 2013; Nalwa,

1994; Li and Y. Zhang, 2005). The changes in morphology and surface area of the CNTs have been observed (Nasir Mahmood *et al.*, 2013; Chakraborty *et al.*, 2006) both before and after purification. Today, the purification of CNTs is a broad field of research. The removal of soluble impurities is easily achieved by washing with toluene or treatment with hot water. However, it is very difficult to separate insoluble impurities. The methods of purification can be classified as follows: The chemical methods, on one hand, are overall oxidation reactions, dynamic air oxidation, and acid treatment (nitric acid is the most often used) (Hou *et al.*, 2002). Physical methods, on the other hand, include direct or tangential microfiltration, and chromatography (Duesberg *et al.*, 1999). In our work, we used nitric acid concentration of 8N for the purification of the MWCNTs. Given MWCNTs remarkable properties, research is being conducted to optimize their applications. By their mechanical resistivity, the CNTs enhance the hardness and resistibility matrices of ceramic materials (William A. Curtin, Brian W. Sheldon). Their adsorption properties allow storage of gasses, particularly

\*Corresponding author: Diana, A.

Condensed Matter and Technology Laboratory, Felix Houphouet Boigny University of Cocody- Abidjan, Côte d'Ivoire.

hydrogen (Gwenaelle Raimbeaux). In recent years, there has been a good deal of experimental and theoretical interest in the possibility of gas storage (hydrogen) in single- and multi-walled carbon nanotubes, as well as carbon fibers. Up to now, a confusing question is where gas resides in these nanostructured carbon materials. It is generally accepted that the majority of hydrogen absorbed in SWCNT was physisorbed on their interior surface, as well as in the interstitial channels between nanotube bundles (Fatemi and Foroutan, 2016). In this work, we studied the adsorption of argon onto MWCNTs with different diameters (60 nm and 110 nm). Our primary concern is to identify at first the adsorption sites of the argon on MWCNTs in order to better understand the gas storage process. Secondly, we seek to understand the effects of the diameters of the MWCNTs on the adsorption of the gas.

**Experimental Section**

**Two types of MWCNTs were used as samples:**

- Sample 1: MWCNT (Aldrich Cat No. 636835-50G) has external diameter: 60-100 nm; internal diameter: 5-10 nm; length: 05-500 microns; purity 95%, pointing CNT\_60.
- Sample 2: MWCNT (Aldrich Cat No. 659258-10G) has an external diameter: 110-170 nm; length: 5-9 microns; purity 90%, pointing CNT\_110.

Knowing the weight, the sample was suspended in nitric acid solution and refluxed at 70° C ± 2° C for 4 h in the case of 4N acid and 24 h in the case of 8N acid. After acid treatment, the samples were separated by filtration and washed thoroughly with deionized water until pH of the filtrate was neutral, dried in air at room temperature followed by drying at 90°C in hot air oven overnight. N<sub>2</sub> adsorption study was carried out at liquid N<sub>2</sub> temperature (~77K) using a surface area analyzer (ASAP 2010C, Micromeritics USA). Surface area was calculated using the Brunauer–Emmett–Teller (BET) model. Total pore volume and average pore diameter were calculated using the Gurvitch method. Pore size distribution analysis was done by the BJH method using the desorption branch of the N<sub>2</sub> isotherm. Micropore area and micropore volume were calculated using the t-plot method (Hou *et al.*, 2002). In addition, a multitude of non-destructive techniques were employed in order to characterize the samples. Detailed microstructural analysis was carried out by transmission electron microscopy (TEM). Moreover, the crystallographic structure was investigated by X-ray diffraction via X’pert MPD diffractometer (Pan Analytical Holland) at 40 kV and 30 mA using monochromatized Cu K radiation (λ = 1.5405 Å) in the 2θ range from 5° to 90.0°. Finally, the argon adsorption study was carried out at liquid N<sub>2</sub> temperature (~77K) using surface area analyzer ASAP 2010C (Micromeritics USA). Argon adsorption capacity and the adsorption energy were calculated. The adsorption capacity refers to the maximum amount of gas that can be adsorbed in the operating conditions per unit mass of the adsorbent. The volumetric storage capacity is expressed by the following expression:

$$C_{ad} = \frac{m_{gas}}{V} \dots\dots\dots(1)$$

- C<sub>ad</sub>: adsorption capacity
- m<sub>gas</sub> : gas mass
- V: volume of pores

The adsorption energy is the energy of interaction between the adsorbent and the adsorbed molecule. It is determined from the following expression:

$$E_{ad} = RT \log C \dots\dots\dots(2)$$

- E<sub>ad</sub>: adsorption energy
- R: gas constant (8.314 J/ K.mol).
- T: temperature (77 K)
- C: constant

C is a constant. It was calculated by the equation below, knowing the slope and the monolayer volume V<sub>M</sub>

$$\alpha = \frac{C-1}{C \times V_M} \dots\dots\dots(3)$$

The study of these parameters will allow us to understand and target the adsorption sites of argon on the surface of MWCNTs. The main output of this work is to answer the following questions:

What is the effect of the diameter of the MWNCT on storage capacity of argon? Which of these two different diameters can store the maximum amount of gas?

**RESULTS AND DISCUSSION**

**Morphology of the samples before and after HNO<sub>3</sub> treatment**

Representative TEM images of the raw and 8N materials (MWCNT-60\_100nm and MWCNT-110\_170nm) used in this study are shown in Figure 1. To our best estimate, the material contained impurities like amorphous carbon, carbon nanoparticles, and a metallic catalyst as indicated with the arrows in Figure 1 a and c. TEM images of the samples after 8N HNO<sub>3</sub> treatment are shown in Figure 1 b and d. Comparing to the raw image, examination of the material at 8N (Figure 1 b and d) confirms the low purity of the sample, it also clearly presents the influence of the HNO<sub>3</sub> on the MWCNT material. The MWCNTs on a composite surface (Figure 1 b and d) with acid treatment are much better in quality than the raw samples (Figure 1 a and c).

**Ar adsorption on MWCNT**

To better understand the phenomenon of hydrogen storage, we conducted a study of the adsorption isotherm of Ar on the MWCNT at liquid nitrogen temperature (77K). We also calculated the adsorption capacity and the adsorption energy from Equations 1 and 2. The results of the experimental analysis are shown in Table 1.

**Effect of diameter**

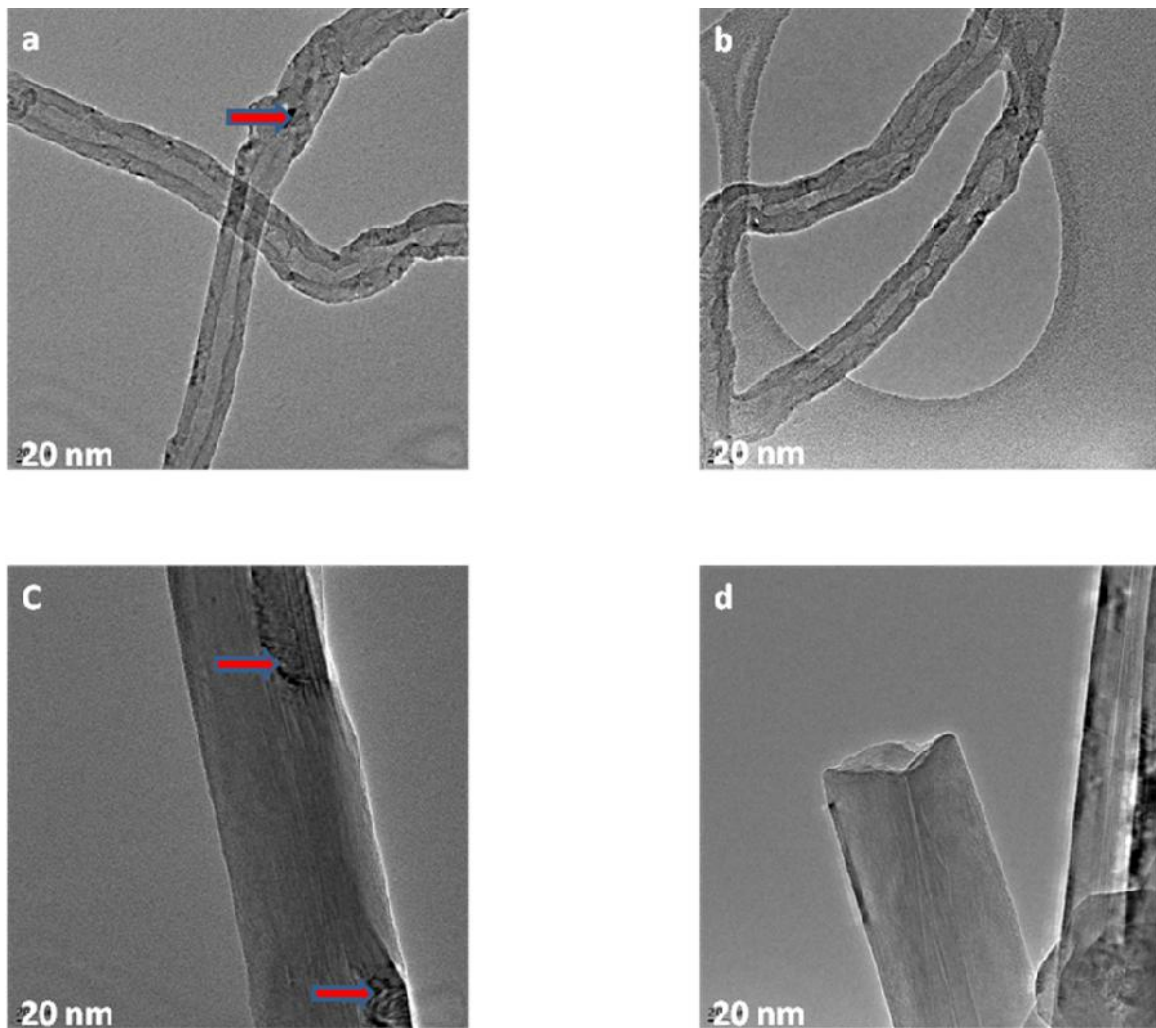
Figure 2 shows the isotherm adsorption of Ar on the MWCNT (CNT\_60 and CNT\_110) purified at 8N at 77K. We represent the number of molecules of Ar adsorbed as a function of P/P<sub>0</sub>.

**Table 1. Summary of experimental results from the adsorption of Ar onto the MWCNT**

	Ar	MWCNT_60	MWCNT_60_8N	MWCNT_110	MWCNT_110_8N
Sample Weight (g)	/	0.0795	0.0943	0.1046	0.1337
outside diameter (nm)	/	60-100	60-100	110-170	110-170
internal diameter (nm)	/	5-10	5-10		
Temperature (K)	77	77	77	77	77
Specific surface area (m <sup>2</sup> /g)		77.1	69.51	10	11.96
Pore volume (cm <sup>3</sup> /g)		0.09	0.14	0.024	0.015
Layer volume (cm <sup>3</sup> /g)		20	18.21	2.6	3.13
Adsorption capacity (wt%)		3.23	2.92	0.43	0.51
adsorption energy (kJ/mol)		3.8184	3.354	3.2648	2.7578

**Table 2. Summary of experimental results of the adsorption of H<sub>2</sub> onto the MWCNT [15]**

	AC	LaNi <sub>3</sub>	MWCNT1	MWCNT2	MWCNT3	MWCNT4
Sample Weight (g)	0.4163	6.1696	0.2013	0.1865	0.1874	0.1836
outside diameter (nm)	/	/	13	24	41	53
internal diameter (nm)	/	/	2-5	2-5	2-5	2-5
specific surface area (m <sup>2</sup> /g) before adsorption	3209	/	178	155	75	24
specific surface area (m <sup>2</sup> /g) after adsorption	/	/	162	155	75	25
Initial pressure (MPa)	13.47	13.52	13.63	13.57	13.52	13.59
equilibrium pressure (MPa)	13.19	10.44	13.31	13.20	13.11	13.15
Temperature(K)	293	293	293	293	293	293
Hydrogen adsorption capacity (wt.%)	0.9	1.4	2.5	3.3	4.0	4.6
Hydrogen desorption capacity (wt. %)	0.8	1.2	1.5	2.1	2.7	3.2
Difference between adsorption and desorption	0.12	0.2	1.0	1.1	1.3	1.4

**Figure 1. (a) Raw TEM image of CNT\_60, (b) TEM image of CNT\_60 at 8N; (C) Raw TEM image of CNT\_110, (d) TEM image of CNT\_110 at 8N**

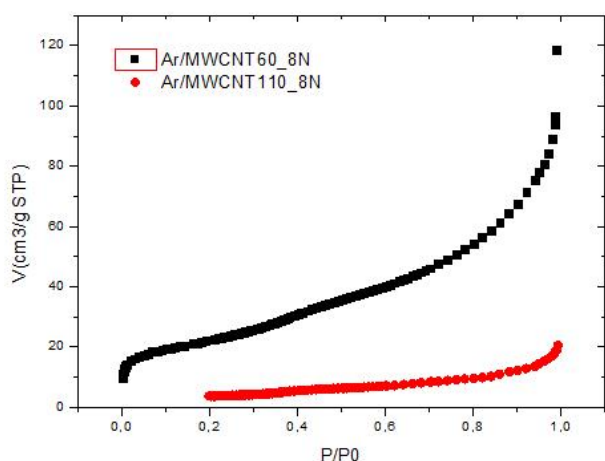


Figure 2. Adsorption of Ar on MWCNT\_60\_8N and MWCNT\_110\_8N at 77 K

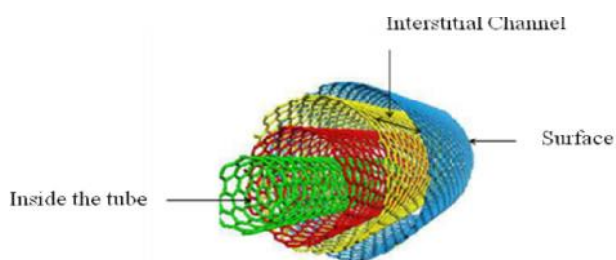


Figure 3. Different adsorption sites

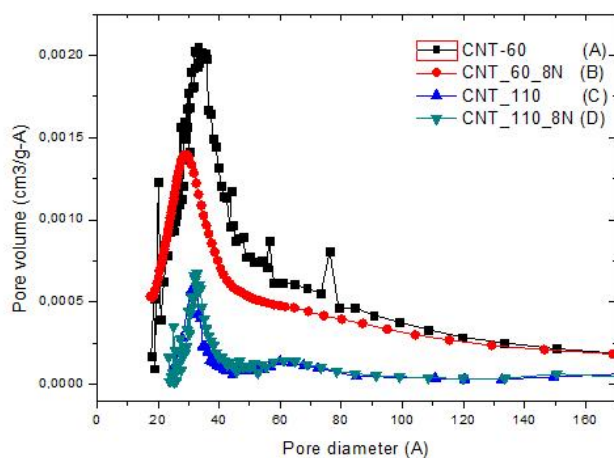


Figure 4. Pore diameters of MWCNTs CNT\_60 and CNT\_110

We observe that the CNT\_60\_8N adsorbs more Ar molecules than CNT\_110\_8N. This can be explained by the fact that the CNT\_60 sample has about 82.8% more surface area than the CNT\_110 sample. That difference may be attributed to the presence of close-end nanotubes in the case of CNT\_110. However, the observed results required further detailed investigation to understand this difference using other techniques like thermal analysis. We also observed that the adsorption capacity and the adsorption energy are inversely proportional to the diameter of MWCNT (Table 1), which is consistent with the results found by Peng-Xiang Hou *et al.* (2003) and Xingbang Hu *et al.* (2011). They concluded that the larger the diameter, the more difficult adsorption onto the

surface of MWCNT becomes. That could be due to the fragility of the bonds between the adsorbent and the adsorbate as the diameter increases. We conclude that adsorption onto the smaller diameter MWCNT is more efficient than for the larger diameter MWCNT.

### Effect of adsorption sites

On MWCNT, gasses can be adsorbed at three different sites. Those are: the surface, the interstitial channels, and within the tubes (Figure 3). Depending on the location of the gas adsorption, different phenomena, either storage or desorption, can occur. Data in Table 1 show that surface area and adsorption capacity are inversely proportional to the diameter of the MWCNT. This is contrary to the work of Peng Hou Xiang *et al.* (2003) in the case of the storage of hydrogen on the MWCNT (Table 2). They concluded that the surface area is inversely proportional to the diameter, but the hydrogen adsorption capacity of the MWCNT is directly proportional to the diameter. If hydrogen was adsorbed only on the surface, the hydrogen adsorption capacity could be increased with the surface area. That allowed them to say that hydrogen can't be stored only on the surface, but is also adsorbed in the inner tube space between adjacent pallets of MWCNT. Here, in the case of argon, the adsorption capacity is directly proportional to the surface area; we deduce that Ar may be only adsorbed onto the surface of the MWCNT, so it would be easily desorbed. Therefore, we conclude that Ar cannot be stored on a MWCNT as can hydrogen.

### Pore Effects

Porosity is important for understanding the gas storage mechanism. During the adsorption phenomenon, the molecules are stored in the pores. The pore structure of our two samples of different diameters is shown in Figure 4. Those four curves have the same shape with a major peak between 20–40 Å. We find that the pore volume decreases with increasing diameter. That reduction suggests that the pores were destroyed by argon adsorption.

### Conclusion

We studied the adsorption of argon onto MWCNTs of two different diameters. We focused on two main objectives: to identify the argon adsorption sites on the MWCNT and to understand the effect of the diameters of MWCNTs on the adsorption. We found from the storage capacity and the surface area that argon is adsorbed onto the surface of the MWCNT. We deduce that argon cannot be stored on MWCNT. We found that as the MWCNT diameter increases, the adsorption energy and the adsorption capacity decrease. Those results disagree with those found in the case of hydrogen adsorption on MWCNT. The difference in diameter influences the number of adsorbed molecules. We suggest improving the storage of hydrogen using MWCNT having smaller diameters. More research is needed to find possible opportunities to achieve storage of other gasses.

### Acknowledgments

The authors are grateful for financial support from INSA-JRD TATA Fellowship D.O. /CCSTDS/1293/2008 and *twas*

Research Grants 08-115/PHYS/AF/AC. We thank professor Aldo. D. Migone and Dr. John S. Graham for providing us helps.

## REFERENCES

- Chakraborty S., J. Chattopadhyay, H. Peng, Z. Chen, A. Mukherjee, R. S. Arvidson, R. H. Hauge and W. E. Billups, 2006. *J. Phys. Chem. B.* 110, 24812.
- Duesberg G. S., W. Blau, H. J. Byrne, J. Muster, M. Burghard, S. Roth, 1999. Chromatography of carbon nanotubes, *Synth. Met.*, 103, 2484-2485.
- Fatemi, S. M. and M. Foroutan, 2016. *Int. J. Environ. Sci. Technol.*, 457-470.
- Hou P.X., S. Bai, Q.H. Yang, C. Liu, H.M. Cheng, Multi-step purification of carbon nanotubes, *Carbon*, 81-85.
- Ijima, S. 1991. *Nature*, 354, 56 - 58.
- Li J. and Y. Zhang, 2005. *Physica E* 28, 309 – 312.
- Mahalingan P., B. Parasuran, T. Maiyalagan, S. Sundaran, *J. Environ. Nanotechnol.*, 1 (2012), 53-61.
- Nalwa, H. S. 1994. *Handbooks of Nanostructured Materials and Nanotechnology*, Academic San Diego, 5, 399.
- Nasir Mahmood, Mohammad Islam, Asad Hameed and Shaikat Saeed, 2013. *Polymer*, 5, 1380-1391.
- Peng-Xiang Hou, Shi-Tao Xu, Zhe Ying, Quan-Hong Yang, C. Liu, Hui-Ming Cheng, carbon, 2003. 2471-2476.
- Salehi E., S. S. Madaeni, L. Rajabi, V. Vatanpour, A. A. Derakhshan, S. Zinadini, S. Ghorabi and H. Ahmadi Monfared, 2012. *Separation and Purification Technology*, 89, 309-319.
- Su X., X. Zhan and B. J. Hinds, 2012. *J. Mater. Chem.*, 22 7979-7984.
- Tu X., Y. Zhao, S. Luo, and L. Feng, 2012. *Microchim. Acta*, 177; 159-166.
- William A. Curtin, Brian W. Sheldon, CNT-reinforced ceramics and metals. Gwenaelle Raimbeaux, porosité gaz/porosité mercure, laboratoire de génie chimique Université de Toulouse, 19, 7-11.
- Xingbang Hu, Chaoying Liu, Youting Wu and Zhibing Zhang, 2011. *New J. Chem.*, 35, 2601-2606.

\*\*\*\*\*